CHEMBIOCHEM

DOI: 10.1002/cbic.200500041

Nanostructured Ordering of Fluorescent Markers and Single Proteins on Substrates

Juergen Groll,*[a] Krystyna Albrecht,[a] Peter Gasteier,[a] Silke Riethmueller,[b] Ulrich Ziener,[b] and Martin Moeller*[a]

*Highly ordered hexagonal nanopatterns of gold clusters on glass substrates were used as anchoring points for the specifc attachment of fluorescence dyes and proteins labeled with fluorescence dyes. Thiol- or disulfide-containing linker molecules were used for the binding to the gold dots. In order to ensure specific binding on the gold dots only, the surface area in between the dots was protected against unspecific adsorption. For the attachment of polar low-molecular-weight fluorescence dyes, an octadecyltrichlorosilane self-assembled monolayer was prepared on the surface in between the gold dots, whereas a layer prepared from star-shaped poly(ethylene oxide-*stat*-propylene oxide) prepolymers was used to prevent unspecific adsorption of proteins between the gold dots. Fluorescence microscopy proved the specific binding of the dyes as well as of the proteins. Scanning force microscopy studies show that each gold dot is only capable of binding one protein at a time.*

Introduction

Immobilization of proteins on surfaces in ordered patterns is a very active field of research.[1–3] In contrast to DNA chips, where the general shape, charge, immobilization chemistry, and detection method are essentially the same for the various oligonucleotides, proteins differ considerably in all these properties. Therefore, the prevention of unspecific interactions and the specific immobilization of different proteins on the molecular level in their native and functional conformations are challenging tasks.[4–6] Technically, despite possibilities like ink-jet technology,[7] photolithography,[8] selective self-assembly,[9] or microcontact printing,[10–12] the production of microarrays is mainly achieved by spotting techniques.[13,14] Attempts to produce patterns with resolutions in the submicron range are harder to realize. Microcontact printing has been used to generate protein patterns with single-protein resolution,[15] but the regularity of the pattern is not perfect. Dip-pen nanolithography[16–18] is a promising method but it is limited to the patterning of very small sample areas. The generation of regular nanopatterns over large surface areas can be accomplished by self-assembly, for example, of block-copolymer micelles on substrates.[19,20] This method enables the generation of gold nanoclusters on substrates in regular hexagonal patterns.[21–23] The applicability of such patterns for biological studies has recently been demonstrated by Spatz and co-workers, who used the gold dots as anchoring points for the specific attachment of cells.[24]

Fluorescent molecules adsorbed on metallic surfaces exhibit strong quenching of their fluorescence due to electromagnetic coupling between the metal and the dye molecules.[25,26] In addition, fluorescence dyes at metal surfaces change their fluorescence rate, their fluorescence lifetime, and their fluorescence yield.[27–29] This process has been studied extensively for metal films, but the situation differs for nanoparticles. Two decisive parameters are the size and geometry of the particles and the distance between the dye molecule and the particle. Whereas a lissamine dye coupled to a gold nanoparticle by a thioether group at a distance of 1 nm exhibits pronounced fluorescence quenching,[30] the fluorescence of the same dye with a longer thioether spacer, which keeps the dye–nanoparticle distance at 2 nm when attached to gold nanoparticles on a solid substrate, resulted in an easily detectable fluorescence intensity.[31] In other work, an unsymmetrical bis(perylene bisimide) dye bearing a disulfide functional group undergoes self-assembly to form aggregated structures on gold surfaces. Intense fluorescence from these dye aggregates is observed on surfaces decorated with hexagonal gold patterns, whereas the fluorescence is only weak on plain gold substrates.[32]

The present study shows the binding of fluorescence dyes and proteins to highly ordered gold-nanodot arrays on substrate surfaces. Since the arrays are prepared by dip-coating into micellar block-copolymer solutions, large sample areas can be patterned easily. The selective immobilization of nitrilotriacetic acid (NTA) groups to the gold dots was visualized by complex formation with nickel(II) chloride and the fluorescence dye Newport Green. To prevent unspecific dye adsorption in this case, the substrate between the gold dots was modified by a hydrophobic octadecyltrichlorosilane (OTS) self-assembled

[a] *Dr. J. Groll, K. Albrecht, P. Gasteier, Prof. Dr. M. Moeller*
Deutsches Wollforschungsinstitut an der RWTH Aachen e.V.
Pauwelsstrasse 8, 52074 Aachen (Germany)
Fax: (+49) 241-802-3301
E-mail: groll@dwi.rwth-aachen.de
moeller@dwi.rwth-aachen.de

[b] *Dr. S. Riethmueller, Dr. U. Ziener*
Department of Organic Chemistry III–Macromolecular Chemistry
University of Ulm
Albert Einstein Allee 11, 89081 Ulm (Germany)

Supporting information for this article is available on the WWW under http://www.chembiochem.org or from the author.

monolayer (SAM). In order to selectively bind avidin–Texas-Red conjugate to the gold dots, *N*-[6-(biotinamido)-hexyl]-3′-(2′-pyridyldithio)propionamide (biotinHPDP) was attached to the gold dots through the disulfide-containing spacer. The surface between the gold dots was modified in this case by a star-shaped poly(ethylene oxide-*stat*-propylene oxide) prepolymer (Star PEG) coating that prevents the unspecific adsorption of proteins and preserves the native conformation of surface bound proteins.[33,34] The selective binding of avidin to the biotin was visualized by fluorescence microscopy and additionally by scanning force microscopy.

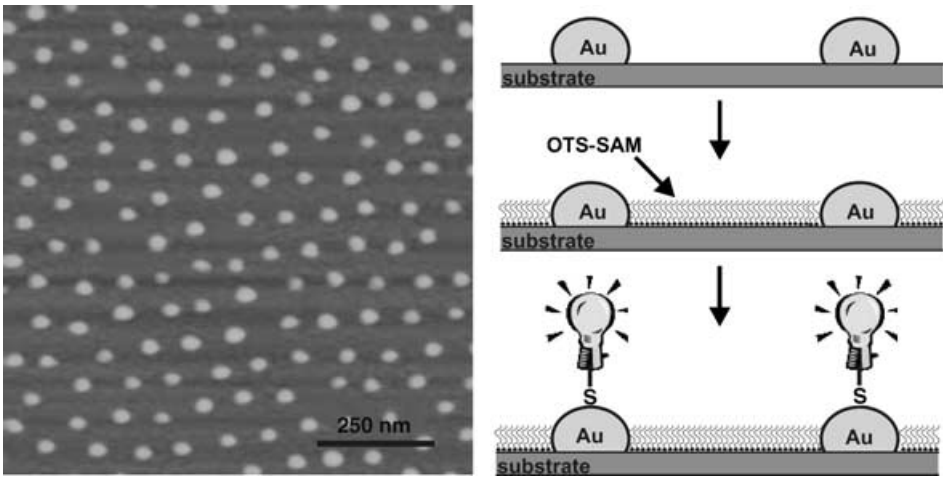

Figure 1. Left: SFM image of a gold-dot-decorated surface derived from $HAuCl_4$-loaded PS(1350)-*b*-P2VP(400) micelles. Right: Illustration of the specific immobilization of fluorescence dyes on such a sample passivated with an OTS SAM to prevent unspecific binding of the fluorescent dye molecules between the gold dots.

Results and Discussion

The preparation of gold-nanoparticle-decorated substrates is based on micellar solutions of poly(styrene)-*block*-poly(2-vinylpyridine) (PS-*b*-P2VP) in toluene. Block-copolymer micelles are size tunable and can easily be used as colloids for the nanostructuring of surfaces.[19–23] The block copolymers self-assemble in selective solvents to form micelles, which serve as compartments for the formation of nanoparticles. The micelles in this study are loaded with $HAuCl_4$. After dipping of the substrate, the resulting monomicellar film can be removed by means of an oxygen or hydrogen plasma. The resulting substrate is decorated by a well-ordered hexagonal pattern of gold nanodots with a narrow size distribution. The size of the gold dots, as well as the distance between the particles, can thereby easily be varied, mainly by alteration of the block lengths of the block copolymer. In order to properly visualize the specific immobilization of the dye molecules on the gold dots, glass substrates were halfway dipped into the gold-salt-loaded solution prior to plasma treatment. The resulting samples are only decorated with gold dots on one half of the sample. After loading of the substrates with the fluorescence dyes, the difference between specific attachment to the gold dots and unspecific dye adsorption can be visualized at the dipping edge where the gold-dot decoration of the substrate ends. The prevention of unspecific adsorption of the polar fluorescent dye molecules was achieved by formation of a SAM of OTS on the area between the gold dots. A SFM image of the gold-dot-decorated surface, as well as arepresentation of the sample-preparation process, is shown in Figure 1.

NTA is widely used as a complexing agent for the purification of recombinant proteins that bear a sequence of histidines (a His tag) at the N or C terminus.[35] Nickel(II) is mainly used as central ion for the complex. Since Ni^{II} forms complexes with octahedral geometry and the NTA group can only fill up four coordination sites, the two empty sites are taken by weakly bound water molecules. If a recombinant protein with a histidine tag approaches this complex, the nitrogen atoms of the imidazole rings replace the water molecules and the protein is immobilized. The complex can later be destroyed by addition of excess imidazole or by complexation of Ni^{II} with ethylenediaminetetraacetate (EDTA). In the case of Newport Green, the nitrogen atoms of the pyridine rings replace the water molecules in the Ni^{II}–NTA complex (Scheme 1).

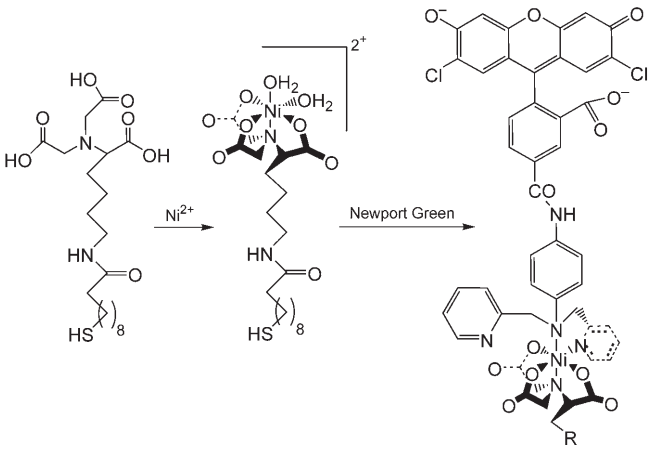

Scheme 1. Immobilization of Newport Green through formation of an octahedral complex with nitrilotriacetic acid and Ni^{II} as the central ion.

Figure 2b shows a fluorescence microscopy image of a glass sample decorated with NTA receptors and subsequently immersed into a nickel(II) chloride solution and a solution of Newport Green in ethanol. The difference between the gold-dot-decorated part of the sample (bottom) and the part without gold dots (top) is clearly visible. As a comparison, a dark-field image of the border area between the gold-dot-covered glass and the unmodified glass of a sample prior to SAM deposition is shown (Figure 2a).

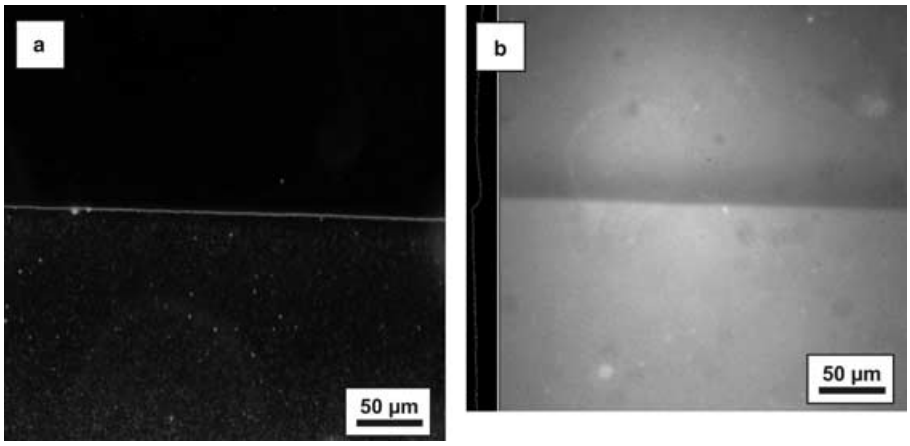

Figure 2. a) Dark-field image of the border area between the gold-dot-covered and unmodified surfaces of a glass sample prior to SAM deposition. b) A fluorescence image of a glass sample after SAM deposition, binding of the NTA to the gold, and complexation with $NiCl_2$ and Newport Green. The line on the left side of (b) shows the fluorescence intensity profile.

In order to immobilize proteins on the gold nanodots, the surface in between the gold dots has to be modified to prevent unspecific protein adsorption. An OTS SAM is not suited for this purpose, since the hydrophobic character of the densely packed alkyl chains rather promotes protein adsorption. Therefore, the area between the gold dots was coated with a Star-PEG layer. We have demonstrated in previous publications that these coatings prevent the unspecific interaction of proteins with the surface.[33,34] With the PS(800)-*b*-P2VP(600) block copolymer used for these experiments, particles with about 10 nm diameter are generated. The idea was not only to prevent unspecific protein adsorption between the gold dots but also to adjust the thickness of the Star-PEG layer in such a way that only the very top of the gold dots is sticking out of the layer. Since proteins are rather big molecules of several nanometers in diameter, it can hence be ensured that only one protein is tethered to one gold dot. An illustration of this model is displayed in Figure 3. To achieve this goal, several gold-dot-decorated samples were coated with different Star-PEG layer thicknesses (Table 1). SFM pictures of gold-dot-decorated glass substrates without Star PEG and with increasing Star-PEG layer thicknesses in between and finally on the gold dots are shown in Figure 4. With increasing Star-PEG layer thickness, the gold dots seem to sink into the surrounding layer; in Figures 4c and 4d, the gold dots are detected as holes in the layer. This shows that the Star-PEG coating dewets the gold dots if possible. Even the 17.7 nm thick coating, which is almost twice as thick as the height of the clusters, contains holes at the positions where the gold dots are covered. The phase images show this even more clearly. These experiments underline the fact that, amongst the other advantages of these coatings, the thicknesses of the Star-PEG layers can be easily controlled.

Table 1. Variation of the concentration of the Star-PEG solutions prior to spin coating and the resulting layer thicknesses.

Star-PEG concentration [mg mL^{-1}]	Layer thickness [nm]
3.0	7.8
5.4	11.2
7.8	17.7

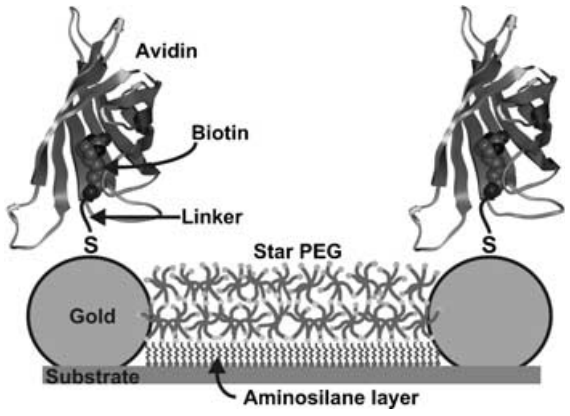

Figure 3. Schematic representation of the coating of the substrate between the gold dots with a Star-PEG film in such a way that only the very top of the gold dots is sticking out. This means that, due to geometric confinement, only one protein is immobilized per gold dot.

The samples as displayed in Figure 4b were chosen for the successive binding of biotinHPDP and the avidin–Texas-Red conjugate to the gold dots, since in this case not much of the dots is sticking out of the layer but they are still accessible for the biotinHPDP molecules. It turned out that the crucial part of the binding procedure is not the binding of the biotinHPDP to the gold or of the avidin–Texas-Red conjugate to the biotin but the washing of the samples after the first step. Obviously, the biotinHPDP gets easily entangled within the Star-PEG network and extensive rinsing of the samples is indispensable in order to prevent protein adsorption between the gold dots. The fluorescence microscopy image of avidin–Texas-Red conjugate bound to the biotin-modified gold dots is presented in Figure 5a. The fluorescence intensity of this image was low, and integration times of 40 s were necessary to obtain unambiguous pictures. Since the distance between the gold dots and the dye molecules is big enough in this system to avoid major quenching effects, the small but homogeneously distributed fluorescence intensity indicates that only a monolayer of dye molecules and hence proteins are present on the gold-dot-decorated part of the substrate. Figures 5b and 5c show height images for this sample monitored by SFM before and after treatment with biotinHPDP and avidin–Texas-Red conjugate. The height profiles reveal that the gold dots after protein immobilization show a height increase of 4–6 nm per gold dot.

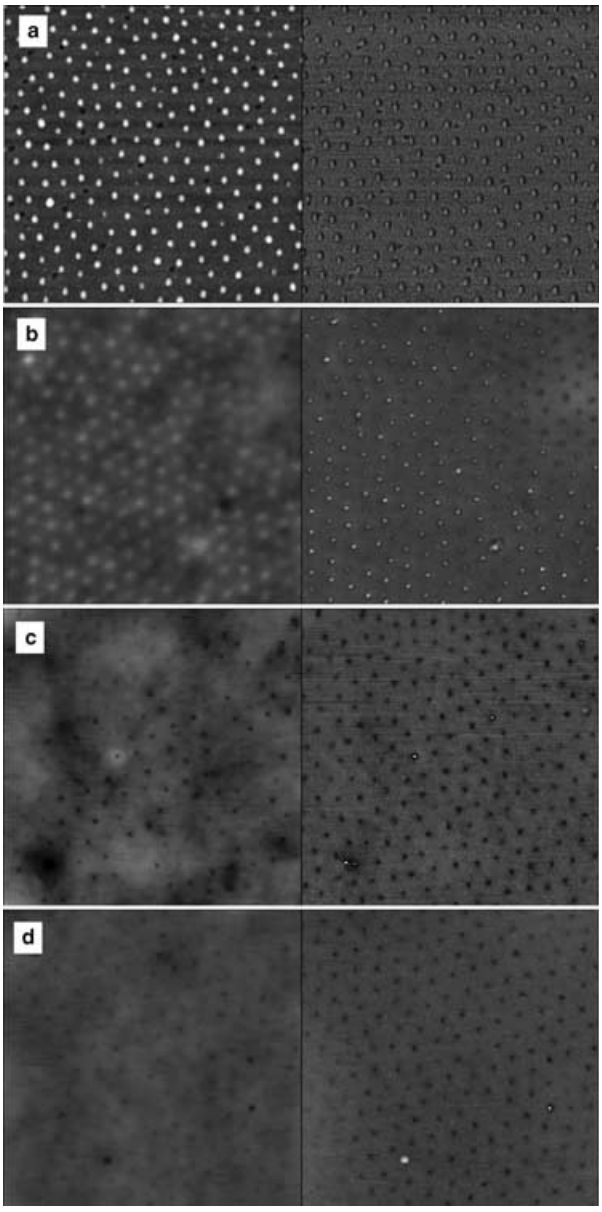

Figure 4. SFM images of a gold-dot-decorated surface derived from PS(800)-*b*-P2VP(600) without further modification (a) or coated with Star-PEG layers of 7.8 (b), 11.2 (c), or 17.7 nm (d) thickness. The scan size is 1 μm. For each thickness, a height image is displayed on the left and a phase image on the right. Layer thicknesses were determined by ellipsometry by film deposition on an aminosilylated silicon wafer from the same solution as that used for the experiments presented here.

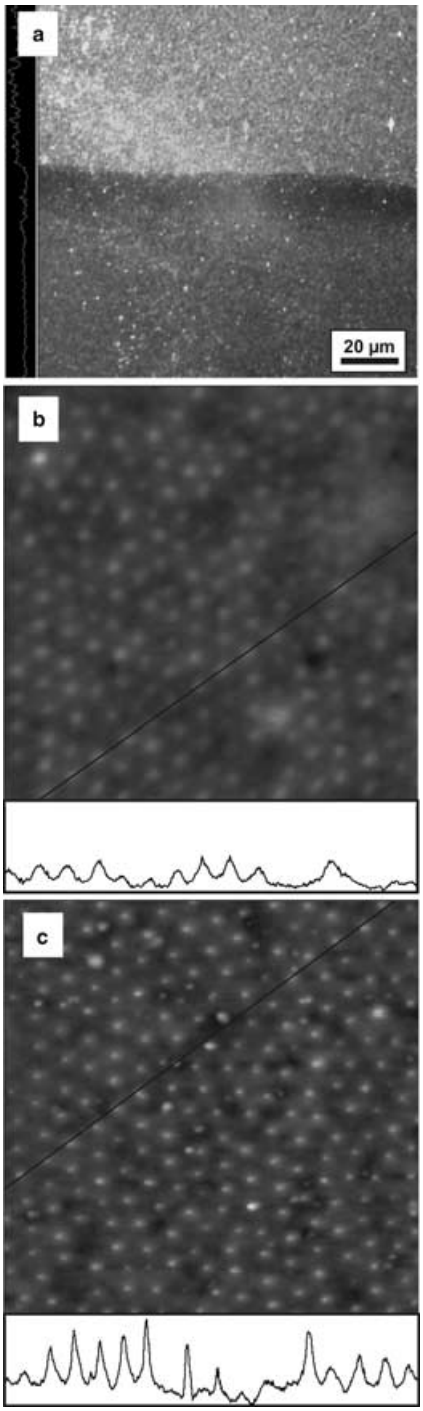

Figure 5. a) Fluorescence microscopy image of the avidin–Texas-Red conjugate tethered to the gold-dot-decorated part of a Star-PEG-modified glass sample through biotinHPDP. The integration time was 40 s, a fact indicating the low fluorescence intensity. b) and c) SFM images (1 × 1 μm) of the gold-dot-decorated part of the sample before (b) and after (c) the binding of avidin. The profile height for both pictures is 10 nm. This indicates selective binding of one avidin per gold dot, since the height increase is 4–6 nm per gold dot.

These numbers correspond to the size of avidin, a result indicating the binding of single proteins to the gold dots. A study with gold-dot patterns at optically resolvable distances that enables direct proof of single-protein attachment to the gold dots by single-molecule fluorescence microscopy is currently in preparation.

Conclusion

This study demonstrates the selective attachment of low-molecular-weight fluorescence dyes and proteins to highly ordered arrays of gold nanodots on surfaces. Depending on the molecules, the substrate area between the gold dots has to be modified to prevent unspecific adsorption. For polar low-molecular-weight molecules such as fluorescence dyes, this can

be accomplished by deposition of a hydrophobic OTS SAM. It was shown that the specific binding can be visualized by fluorescence dyes, although the gold nanoparticles partially quench the fluorescence. Experiments with proteins require other surface modifications that prevent unspecific adsorption, such as Star-PEG layers. This system has the advantage of easy adjustability of layer thickness, so that gold-dot-decorated glass samples could be coated with Star PEG in such a way that only the very top of the gold dots was sticking out. Fluorescently labeled avidin was tethered to the gold dots of such a sample through biotinHPDP. The resulting fluorescence microscopy image shows specific binding of avidin to the gold dots, and the low intensity supports the assumption that only one protein is bound per gold dot. In addition, SFM studies on substrates before and after protein attachment also indicate the binding of individual proteins on the gold dots. Since the distance between the gold dots can be increased to distances that are accessible to optical methods, these results enable applications for this system such as nanoarrays of individually addressable proteins and the analysis of single proteins that are immobilized on the surface.

Experimental Section

Materials: Six-armed star-shaped isocyanate-terminated PEG prepolymers have been obtained from SusTech and used as received. The poly(styrene)-*block*-poly(2-vinylpyridine) block copolymers PS(800)-*b*-P2VP(600) and PS(1350)-b-P2VP(400) were synthesized by living anionic polymerization.[22] Tetrachloroauric acid ($HAuCl_4 \cdot 3H_2O$, Fluka, pure), nickel(II) chloride hexahydrate (Aldrich, 99.9998%), Newport Green dipotassium salt (Molecular Probes, 78%), trifluoroacetic acid (Merck, >98%), and phosphate-buffered saline (PBS) tablets (Sigma) were used as received. Acetone and isopropanole (Merck, selectipure) were stored in a class 100 clean-room and used as received. Tetrahydrofuran (THF) and toluene (Aldrich, p.A.) were distilled from $LiAlH_4$. Octadecyltrichlorosilane (OTS; ABCR, 98%) was filtered prior to use. *N*-[6-(Biotinamido)-hexyl]-3′-(2′-pyridyldithio)propionamide (BiotinHPDP; Pierce) was stored at −20 °C and used as received. Avidin–Texas-Red conjugate (Molecular Probes) was stored at −20 °C. Solutions were made in PBS buffer (pH 7.4) with a concentration of 20 μg mL^{-1} prior to use.

Methods: SFM investigations were performed with a nanoscope III instrument (Digital Instruments, Santa Barbara, CA, USA) operating in Tapping ModeTM. The oscillation frequency for Tapping ModeTM was set in the range of 320–360 kHz depending on the Si cantilever ($k \approx 50$ N m^{-1}; Nanosensors, Neuchâtel, Switzerland). Dip coating was performed by means of a homemade dipping device. Microwave plasma etching experiments were carried out in a TePla 100 plasma etcher (TePla AG, Asslar Germany). Layer thicknesses were examined by using a spectral MM-SPEL-VIS ellipsometer (OMT, Ulm, Germany). Measurements were performed in the wavelength range from 450–900 nm. The azimuthal angle was kept at 15°, and the integration time was dependent on the layer thickness as well as the resulting signal intensity. Ultraflat D263T glass plates with a thickness of 170 μm were purchased from Schott-Desag AG (Grünenplan, Germany). Fluorescence microscopy was performed by using an Axioplan2 Imaging microscope (Zeiss, Oberkochen, Germany) combined with an NXBO75 lamp (Zeiss) and the Zeiss fluorescence filter set 31 for avidin–Texas-Red conjugate. For Newport Green, the filter set F41–018 from AHF Analysentechnik AG (Tübingen, Germany) was used. Pictures were taken with a NTE/CCD 512EBFT camera (Princeton Instruments, Trenton, NJ, USA). The intensity for fluorescence measurements is given as counts per second (cps).

Preparation of the micellar solution: A 0.5 wt% solution of the block copolymer in dry toluene was mixed with 0.5 of an equivalent of $HAuCl_4 \cdot 3H_2O$ per pyridine unit. The mixture was stirred for at least 24 h to allow complete solubilization of the tetrachloroauric acid in the cores of the block copolymer micelles. Prior to dip coating, the solution was filtered through a syringe filter with 1 μm pore size.

Preparation of dipcoated films: The preparation of samples was carried out in a class 100 clean-room. Glass samples were cut to 10×15 mm pieces and cleaned by sonication in acetone, water, and isopropanole for 1 min each. After activation by oxygen plasma (110 W, 10 min, 0.5 mbar), the substrates were fixed on a substrate holder, dipped halfway into the micellar solution with a velocity of 16 mm min^{-1}, and pulled out of the solution with the same velocity. After solvent evaporation, the samples were subsequently treated with oxygen plasma (110 W, 30 min, 0.5 mbar) on both sides. The samples were then stored under clean-room conditions until further use. PS(1350)-*b*-P2VP(400) was used to generate gold-dot patterns for attachment of fluorescence dyes. Samples for specific avidin immobilization were prepared from PS(800)-*b*-P2VP(600).

Passivation of the samples with OTS SAMs: All glassware used for monolayer preparation was immersed in freshly prepared piranha acid. Subsequently, the glassware was stored in Millipore water. The water was changed every 3 h until the pH value stayed above 5.5. The glassware was then dried and stored under clean-room conditions. The gold-dot-decorated substrates were treated with UV/ozone for 12 min, transferred into a glove box, and immersed into a 10^{-3} M solution of octadecyltrichlorosilane in dry toluene.[36,37] After 12 h, monolayer formation was finished and the substrates were removed from the solution, extensively rinsed with dry toluene, and stored in dry toluene.

Passivation of the samples with Star PEG: Activation and aminosilylation of the substrates, as well as spincoating of Star-PEG(12000) prepolymer solutions in water/THF (9:1), was done according to the procedures published earlier.[33,34] In order to obtain Star-PEG layers with different thicknesses, the concentration of the Star-PEG solutions prior to spin coating was varied (Table 1).

Attachment of the NTA thiol to OTS passivated samples: Gold-dot-decorated samples passivated by an OTS SAM on the glass surface between the gold dots were immersed into an aqueous solution of the NTA thiol over night. After extensive rinsing of the samples with Millipore water, the samples were immersed into a solution of nickel(II) chloride (50 mg) in Millipore water (10 mL) for 10 min. The samples were then rinsed again several times with Millipore water and immersed into a solution of Newport Green (5 mg) in ethanol (15 mL). After thorough rinsing with ethanol, the samples were dried in a stream of nitrogen and examined by fluorescence microscopy.

Attachment of BiotinHPDP to Star-PEG passivated samples: Gold-dot-decorated samples passivated by Star PEG on the glass surface between the gold dots were immersed into a solution of 5 mg BiotinHPDP in *N*,*N*-dimethylformamide (DMF, 10 mL) overnight. The samples were then gently shaken in absolute DMF at 50 °C for 3 days. The DMF was changed several times per day. The samples were then rinsed once with DMF and three times with Mil-

lipore water and dried in a stream of nitrogen. The samples were then immersed into a solution of avidin–Texas-Red conjugate in PBS buffer (20 $\mu g\,mL^{-1}$, pH 7.4) for 20 min. After rinsing with PBS buffer several times, the samples were dried in a stream of nitrogen and examined by fluorescence microscopy.

Acknowledgements

SusTech (Darmstadt, Germany) is gratefully acknowledged for providing Star PEG prepolymers and for support with the Star PEG technology.

Keywords: molecular recognition · monolayers · nanostructures · protein adsorption · single molecules

[1] J. Glökler, P. Angenendt, *J. Chromatogr. B: Anal. Technol. Biomed. Life Sci.* **2003**, *797*, 229 – 240.
[2] P. Mitchell, *Nat. Biotechnol.* **2002**, *20*, 225 – 229.
[3] D. S. Wilson, S. Nock, *Angew. Chem.* **2003**, *115*, 510 – 517; *Angew. Chem. Int. Ed.* **2003**, *42*, 494 – 500.
[4] W. Kusnezow, J. D. Hoheisel, *J. Mol. Recognit.* **2003**, *16*, 165 – 176.
[5] P. Angenendt, J. Glökler, D. Murphy, H. Lehrach, D. J. Cahill, *Anal. Biochem.* **2002**, *309*, 253 – 260.
[6] P. Angenendt, J. Glökler, J. Sobek, H. Lehrach, D. J. Cahill, *J. Chromatogr. A* **2003**, *1009*, 97 – 104.
[7] L. Pardo, W. C. Wilson, Jr., T. Boland, *Langmuir* **2003**, *19*, 1462 – 1466.
[8] H. Sorribas, C. Padeste, L. Tiefenauer, *Biomaterials* **2002**, *23*, 893 – 900.
[9] R. Michel, J. W. Lussi, G. Csucs, I. Reviakine, G. Danuser, B. Ketterer, J. A. Hubbell, M. Textor, N. D. Spencer, *Langmuir* **2002**, *18*, 3281 – 3287.
[10] J. L. Tan, J. Tien, C. S. Chen, *Langmuir* **2002**, *18*, 519 – 523.
[11] H. D. Inerowicz, S. Howell, F. E. Regnier, R. Reifenberger, *Langmuir* **2002**, *18*, 5263 – 5268.
[12] J. Hyun, Y. Zhu, A. Liebmann-Vinson, T. P. Beebe, A. Chilkote, *Langmuir* **2001**, *17*, 6358 – 6367.
[13] G. MacBeath, S. L. Schreiber, *Science* **2000**, *289*, 1760 – 1763.
[14] B. B. Haab, M. J. Dunham, P. O. Brown, *GenomeBiology* **2001**, *2*, 0004.1 – 0004.13.
[15] J. P. Renault, A. Bernard, A. Bietsch, B. Michel, H. R. Bosshard, E. Delamarche, M. Kreiter, B. Hecht, U. P. Wild, *J. Phys. Chem. B* **2003**, *107*, 703 – 711.
[16] K.-B. Lee, S.-J. Park, C. A. Mirkin, J. C. Smith, M. Mrksich, *Science* **2002**, *295*, 1702 – 1705.
[17] J. Hyun, S. J. Ahn, W. K. Lee, A. Chilkoti, S. Zauscher, *Nano Lett.* **2002**, *2*, 1203 – 1207.
[18] J.-H. Lim, D. S. Ginger, K.-B. Lee, J. Heo, J.-M. Nam, C. A. Mirkin, *Angew. Chem.* **2003**, *115*, 2411 – 2414; *Angew. Chem. Int. Ed.* **2003**, *42*, 2309 – 2312.
[19] J. C. Meiners, A. Ritzi, M. H. Rafailovich, J. Sokolov, J. Mlynek, G. Krausch, *Appl. Phys. A* **1995**, *61*, 519 – 524.
[20] A. Roescher, M. Möller, *Adv. Mater.* **1995**, *7*, 151 – 154.
[21] J. P. Spatz, S. Sheiko, M. Möller, *Macromolecules* **1996**, *29*, 3220 – 3226.
[22] J. P. Spatz, S. Mößmer, C. Hartmann, M. Möller, T. Herzog, M. Krieger, H.-G. Boyen, P. Ziemann, B. Kabius, *Langmuir* **2000**, *16*, 407 – 415.
[23] M. Haupt, S. Miller, K. Bitzer, T. Thonke, R. Sauer, J. P. Spatz, S. Mößmer, C. Hartmann, M. Möller, *Phys. Status Solidi B* **2000**, *224*, 867 – 870.
[24] M. Arnold, E. A. Cavalcanti-Adam, R. Glass, J. Blümmel, W. Eck, M. Kantlehner, H. Kessler, J. P. Spatz, *ChemPhysChem* **2004**, *5*, 383 – 388.
[25] V. H. Drexhage in *Progress in Optics XII* (Ed.: E. Wolf), North Holland, Amsterdam, **1974**, pp. 163 – 232.
[26] R. R. Chance, A. Prock, R. Silbey, *Adv. Chem. Phys.* **1978**, *37*, 1.
[27] E. Dulkeith, A. C. Morteani, T. Niedereichholz, T. A. Klar, J. Feldmann, S. A. Levi, F. C. J. M. van Veggel, D. N. Reinhoudt, M. Möller, D. I. Gittins, *Phys. Rev. Lett.* **2002**, *89*, 203002 1 – 2003002 4.
[28] S. A. Levi, A. Mourran, J. P. Spatz, F. C. J. M. van Veggel, D. N. Reinhoudt, M. Möller, *Chem. Eur. J.* **2002**, *8*, 3808 – 3814.
[29] T. Huang, R. W. Murray, *Langmuir* **2002**, *18*, 7077 – 7081.
[30] B. Dubertret, M. Calame, A. J. Libchaber, *Nat. Biotechnol.* **2001**, *19*, 365 – 370.
[31] C. Fan, S. Wang, J. W. Hong, G. C. Bazan, K. W. Plaxco, A. J. Heeger, *Proc. Natl. Acad. Sci. USA* **2003**, *100*, 6297 – 6301.
[32] U. Haas, J. Adams, J. Fuhrmann, S. Riethmüller, U. Beginn, U. Ziener, M. Möller, C. Thalacker, R. Dobrawa, F. Würthner, *J. Mater. Chem.* **2003**, *13*, 767 – 772.
[33] J. Groll, E. V. Amirgoulova, T. Ameringer, C. D. Heyes, C. Röcker, G. U. Nienhaus, M. Möller, *J. Am. Chem. Soc.* **2004**, *126*, 4234 – 4239.
[34] E. V. Amirgoulova, J. Groll, C. D. Heyes, T. Ameringer, C. Röcker, M. Möller, G. U. Nienhaus, *ChemPhysChem* **2004**, *5*, 552 – 555.
[35] E. Hochuli, H. Döbeli, A. Schacher, *J. Chromatogr.* **1987**, *411*, 177 – 184.
[36] K. H. Drexhage, M. Fleck, H. Kuhn, F. P. Schäfer, *Ber. Bunsen-Ges. Phys. Chem.* **1966**, *20*, 1179 – 1183.
[37] H. Kuhn, *J. Chem. Phys.* **1970**, *53*, 101 – 108.

Received: January 31, 2005

